Tribol Lett
DOI 10.1007/s11249-013-0129-7

ORIGINAL PAPER

Tribological Thermostability of Carbon Film with Vertically Aligned Graphene Sheets

Cheng Chen · Dongfeng Diao

Received: 27 November 2012 / Accepted: 10 March 2013

Abstract Tribological thermostability of carbon film with vertically aligned graphene sheets was studied with annealing temperatures up to 1,750 °C. The carbon film was deposited on silicon carbide substrate by electron cyclotron resonance plasma sputtering. Tribological thermostabilities of the carbon film in terms of friction coefficient, wear life, and nanoscratch depth were investigated by Pin-on-Disk tribometer and atomic force microscopy. The evolution of nanostructure of vertically aligned graphene sheets in the carbon film as a function of annealing temperature was examined by Raman spectroscopy and transmission electron microscopy. The results showed that the friction coefficient, wear life, and nanoscratch depth of the carbon film were thermally stable up to 1,250 °C. When the annealing temperature was 1,500 °C, the friction coefficient and the nanoscratch depth increased, the wear life decreased, but still all were of considerable values. These variations were attributed to the initiation of tubular-like structure originated from graphene sheets stacks. After annealing at 1,750 °C, tribological performances degraded catastrophically due to the abundant formation of tubular-like structures and the appearance of a graphitic interlayer between the film and the substrate.

C. Chen · D. Diao (✉)
Key Laboratory of Education Ministry for Modern Design and Rotor-Bearing System, School of Mechanical Engineering, Xi'an Jiaotong University, Xi'an 710049, China
e-mail: dfdiao@mail.xjtu.edu.cn

D. Diao
Nanosurface Science and Engineering Research Institute, College of Mechatronics and Control Engineering, Shenzhen University, Shenzhen 518060, China

Keywords Carbon film · Graphene sheet · Tribological thermostability · Nanoscratch · Friction coefficient · Wear life

1 Introduction

Carbon-based thin films have been developed to address a broad range of coating applications, including uses that demand outstanding tribological performances (low friction coefficient, long wear life) in a wide variety of operating environments [1–3]. Thermostability of the tribological property is an important practical property of carbon-based films. A higher tribological thermostability indicates a wider range of applicable temperature. Many researchers have studied the thermal annealing effect on the tribological properties of different carbon-based films. In general, thermostability of carbon-based films is limited by the instability of sp^3 bonds and the bonds between carbon and doping elements, of which effects are to improve the properties of carbon-based films with higher hardness and lower friction. At temperatures higher than 200 °C, annealing causes the effusion of hydrogen and the transformation from sp^3 bonds to sp^2 bonds in hydrogenated diamond-like carbon film, leading to more graphite-like structure of lower hardness and higher wear rate [4]. Nitrogen is desorbed out of the carbon nitride film at 400 °C and the film microstructure favors a graphitization [5]. For the tetrahedral amorphous carbon film, large numbers of sp^3 bonds convert to sp^2 bonds at above 1,100 °C [6, 7]. These indicate that the thermal unstable bonds in the carbon-based films determine the annealing temperature for graphitization, which results in degradation of tribological performance. And it limits the application development of carbon-based films in high operating temperature environments, such as glass industry

Published online: 22 March 2013

and aerospace industry. It is well-known that sp^2 bond is more stable than sp^3 bond. Therefore, carbon films, of which excellent tribological property and high hardness mainly relies on the sp^2 bonds nanostructure, can be expected with a higher thermostability.

Recently, carbon film with oriented graphene sheets, which contains a high content of sp^2 bonds, has attracted lots of theoretical and experimental attentions since it shows not only good nanoscratch performance comparable to that of diamond but also outstanding directional thermal and electrical properties [8–14]. This kind of carbon film is of high value in potential applications of electronics and thermal management [15, 16]. Since sp^2 bonds are dominant in the film, a higher thermostability can be expected than other carbon-based films. However, related researches on the film are quite few. Shigeki Tsuchitani et al. [17] have studied the structural evolution of this kind of carbon film upon thermal annealing, and found that the basic structure of the film was maintained with a small increase in the size of sp^2 nanocrystallites and a lowering of disorder after annealing up to 700 °C. But there are no researches reporting the annealing effects on this kind of film at the temperature above 1,100 °C. And the dependence of tribological thermostability on the size of sp^2 nanocrystallite at higher temperature is not clear.

In this paper, we prepared carbon film with vertically aligned graphene sheets by electron cyclotron resonance (ECR) plasma sputtering. And the carbon films were annealed in argon gas at temperatures in the range of 1,000–1,750 °C to study the thermostability of the tribological properties. Nanoscratch depth of the carbon film was evaluated with atomic force microscopy (AFM). The friction coefficient and wear life were obtained by a Pin-on-Disk tribometer. The evolution of vertically aligned graphene sheets nanostructure in the carbon film was examined by Raman spectroscopy and transmission electron microscopy (TEM). The film composition was analyzed by X-ray photoelectron spectroscopy (XPS). Electrical conductivity of the film was measured with four-point-probe method. The relationship between tribological properties and corresponding nanostructure was discussed at different annealing temperatures.

2 Experiments

2.1 Preparation and Annealing Treatment of Carbon Films

Carbon films were deposited onto Si-face 4H-N SiC (0001) wafers (resistivity of 0.023 Ω cm) by ECR-sputtering [18–20]. Silicon carbide wafers were cut into 10 × 10 mm squares and fixed onto the substrate holder after cleaned in acetone and ethanol bath by ultrasonic wave. Argon gas pressure was 6.3×10^{-2} Pa and microwave power was 500 W. Before deposition, the substrate surface was cleaned by argon ion sputtering for 3 min. During deposition, a sputtering bias voltage of −500 V was applied onto carbon target. The substrate bias voltage was set as −100 V and the irradiation ion current density was 5.8 mA/cm^2. The duration of deposition was kept to 15 min and the film thickness was 50 nm. No substrate heating was performed during the deposition.

Carbon films were thereafter annealed at 1000, 1250, 1500, and 1750 °C in a carbon heater electrical furnace under 1 L/min flowing argon gas. The films were heated from room temperature (RT) to 600 °C in 20 min, then were heated to the determined temperatures in 3 min, and were kept at the determined temperatures for 10 min. The samples were naturally cooled to RT after annealing.

2.2 Tribological and Nanostructural Characterizations

The tribological experiments of the films sliding against a Si_3N_4 ball (radius of 3.17 mm) were performed with a Pin-on-Disk tribometer. The normal load was 2 N and the sliding velocity was 19 mm/s, corresponding to a constant disk rotational speed of 180 rpm with a frictional circle radius of 1 mm. In order to reduce experimental error, five repeated tribotests were carried out for each film annealed at different temperatures. All tests were operated at RT with a relative humidity of 40–50 %. The nanoscratch depths of the carbon films were evaluated with nanoscratch test using an AFM. A stainless steel cantilever (length: 2.4 mm, width: 200 μm, thickness: 40 μm, stiffness: 43.8 N/m) with a three-sided pyramidal diamond tip was attached to the cantilever holder of the AFM. The tip radius of curvature is 80 nm, which was confirmed with a scanning electron microscope. The cantilever normal force is derived by multiplying the cantilever normal bending by the normal bending elastic constant of the cantilever of 43.8 N/m. The calibration of the normal bending elastic constant of the cantilever was carried out in a commercial nano-indentation tester by deflecting the cantilevers under preset loads. The sample surfaces were scanning-scratched with the diamond tip at a high contact load (30 μN) over a small scanning area (1 × 1 μm) for one pass, and then the surface topographies were measured with the same tip at a low contact load (1 μN) over an enlarged scanning area (5 × 5 μm). The wear depths were measured using the sectional information of the scratched areas of the surfaces. The Hertzian contact pressure in the AFM nanoscratch test is 25.7 GPa, which is about 33 times higher than that in the Pin-on-Disk tribotest.

Raman spectra were obtained with HORIBA HR800 laser confocal Raman spectrometer using a 514 nm laser

for excitation. The laser spot was 2 μm and the laser power was 2 mW to avoid heating damage to the samples. The nanostructures of graphene sheets stacks in the carbon films were further characterized by a JEM-2100 TEM operated at 200 kV. Samples for plan view were prepared by scratching the film surfaces with a diamond pencil, and the flakes were transferred onto copper micro grids. Samples for cross sectional view were prepared by conventional mechanical polishing followed by ion beam milling. The variation of chemical components of the films caused by thermal annealing was investigated by an AXIS ultra DLD multifunctional XPS. The electrical conductivities of the carbon films were measured by four-point-probe method.

3 Results

3.1 Tribological Thermostability of Carbon Film

Figure 1 shows the typical friction curves of the as-deposited carbon film and carbon films after annealing at 1000, 1250, and 1500 °C. For the as-deposited carbon film, the friction coefficient was about 0.158 at the beginning, and decreased immediately to the stable value of 0.046 after about 500 sliding cycles. When the frictional cycle reaches 4,900 cycles, a sudden rise in fluctuation of friction coefficient appeared in the friction curve. Meanwhile, the corresponding worn surface of the carbon film showed some damages in an optical microscope. The number of sliding cycles was defined as the wear life of the carbon film. After annealing at 1,000 and 1,250 °C, more sliding cycles (about 800 and 1,000 cycles, respectively) were needed for the friction to reach stable. And the values of low friction coefficient kept at approximate 0.05. At 1,500 °C, the friction coefficient stayed at a high value of about 0.174 without a low stable stage before the film was worn out. The friction curve of the film annealed at 1,750 °C is not shown in the figure, because the spalling of the film was observed at the very beginning of the friction test.

Wear life and nanoscratch depth are important parameters in evaluating the wear resistance of carbon film in macroscopic and nano scale. Normally, a lower nanoscratch depth indicates a better anti-wear property. Figure 2a shows the evolutions of wear life and nanoscratch depth of the carbon film as functions of annealing temperature. A typical nanoscratched surface of the carbon film annealed at 1,000 °C is shown in Fig. 2b. It can be seen that the wear life and nanoscratch depth of the carbon film stayed relatively constant up to 1,250 °C, and remained considerable values at 1,500 °C. While at 1,750 °C, the wear life decreased and nanoscratch depth increased sharply. Thus, it can be concluded that the tribological properties of the carbon film are thermally stable up to 1,250 °C.

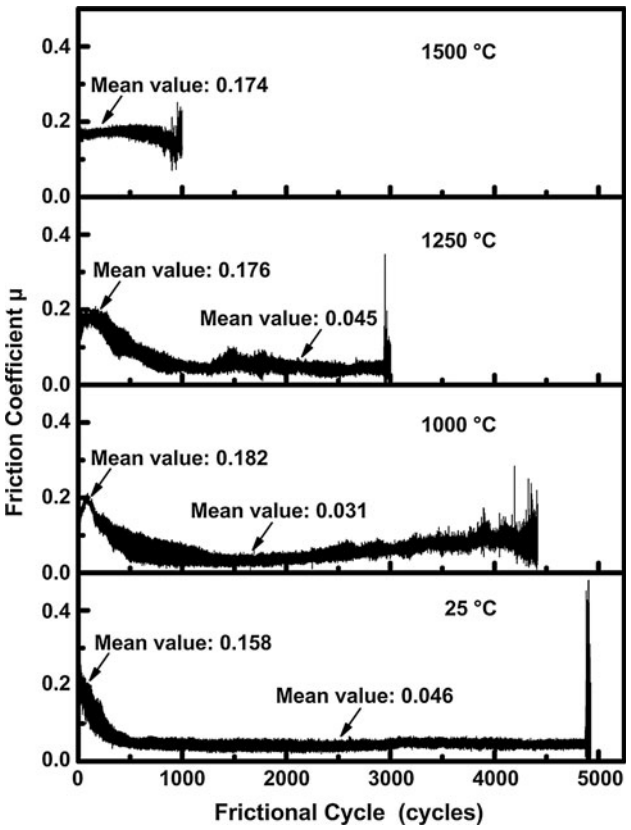

Fig. 1 Friction curves of the carbon films annealed at different temperatures

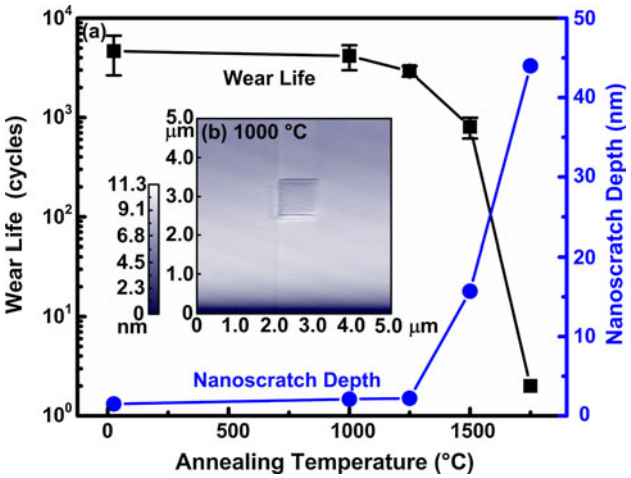

Fig. 2 *a* Wear life and nanoscratch depth of the carbon films as functions of annealing temperature. *b* Nanoscratched surface of the carbon film annealed at 1,000 °C. The thickness of the carbon film is 50 nm

3.2 The Evolution of Nanostructure of Vertically Aligned Graphene Sheets

Figure 3 shows the analysis results of Raman spectroscopy. Raman spectra of the carbon films after annealing at

different temperatures are shown in Fig. 3a. In the region ranging from 1,100 to 2,000 cm^{-1}, each spectrum consists of three main bands at around 1340, 1520, and 1590, which are assigned to D band, SiC band, and G band, respectively. The D band is due to the breathing modes of sp^2 carbon atoms in clusters of six-membered rings. The SiC band arises from Si–C vibrations in the underlying silicon carbide substrate. The G band is attributed to in-plane bond-stretching motion of pairs of the sp^2 carbon atoms. D band and SiC band were fitted with two Lorentzians, while G band was fitted with a Breit-Fano-Wagner (BFW) line as shown in Fig. 3b. Figure 3c shows the peak intensity ratio of the D band to G band (I_D/I_G) and G-band position as functions of annealing temperature. It can be seen that I_D/I_G increased gradually from 0.48 for the as-deposited film to 1.25 for the film annealed at 1,750 °C. G-band position shifted from 1,533 cm^{-1} for the as-deposited film up to maximum ($\sim$1,600 cm^{-1}) at 1,250 °C, then kept constant up to 1,750 °C. Ferrari and Robertson [21] proposed a three-stage amorphization trajectory ranging from graphite to tetrahedral amorphous carbon (ta-C) as a function of the G-band position and I_D/I_G ratio. According to the three-stage amorphization trajectory, the as-deposited carbon film and carbon films after annealing at different temperatures are in stage 2 ranging from amorphous carbon type to nanocrystalline graphite type. And the size of sp^2 clustering in the carbon film increased gradually with annealing temperature.

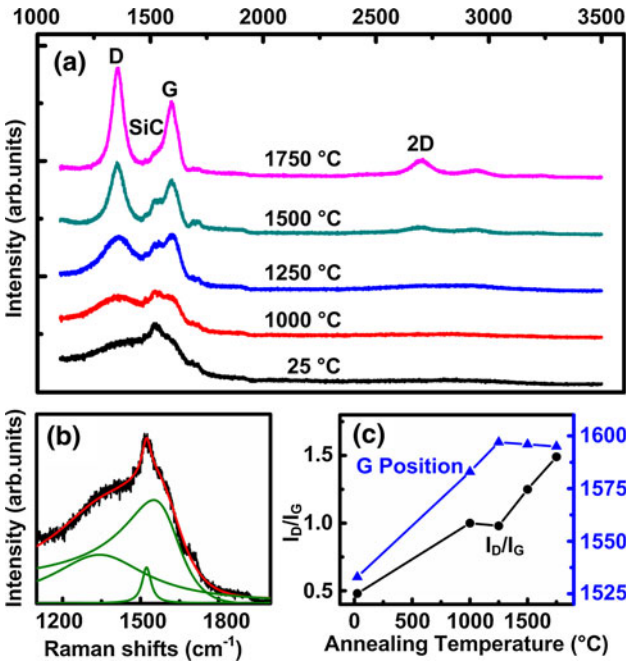

Fig. 3 Analysis results of the Raman spectroscopy. **a** Raman spectra of the as-deposited carbon film and those annealed at different temperatures. **b** A representative peak fitting result of Raman spectrum (as-deposited film). **c** Variations of I_D/I_G and G-band position as functions of annealing temperature

Moreover in Fig. 3a, when the annealing temperatures are at 1,500 and 1,750 °C, a band centered near 2,700 cm^{-1} can be observed. This band is normally named 2D, and it is often observed in graphene or graphite samples [22]. So the appearance of this band indicated that the size of sp^2 clustering may increase to a critical state at 1,500 °C.

In order to better study the effect of thermal annealing on the nanostructure of sp^2 clustering in carbon film, TEM was used and the results are shown in Figs. 4 and 5. In the cross sectional view TEM image of the as-deposited carbon film (Fig. 4a), 1–3 nm-scale graphene sheets stacks were distributed in the amorphous matrix. The orientation of graphene sheets was perpendicular to the substrate. While the graphene sheets stacks could not be identified in the plan view TEM image (Fig. 4b). After annealing at 1,000 and 1,250 °C, the size of graphene sheets stacks increased slightly in the cross sectional view TEM images (Fig. 4c, e). And plan view TEM images (Fig. 4d, f) still show no obvious graphene sheets stacks in carbon film. At 1,500 °C, few tubular-like structures appeared in the carbon film, as shown in Fig. 4g, h. This indicates that the nanostructure of graphene sheets stacks might reach a critical transition state and initially developed to be tubular-like. This result is consistent with the appearance of 2D band observed in Raman spectra at 1,500 °C. When the annealing temperature was increased up to 1,750 °C, abundant tubular-like structures were formed in the carbon film, as shown in Fig. 5b, c. Meanwhile, a 10 nm-thick graphitic interlayer with graphitic fringes parallel to the substrate appeared between the film and the substrate, as shown in Fig. 5a, d. The formation of the graphitic interlayer was caused by evaporation of Si atoms from the SiC substrate [23]. This remarkable structural change in the carbon film and the formation of the graphitic interlayer resulted in an increasing intensity of 2D band observed in Raman spectra (see Fig. 3a).

Figure 6 shows the C 1 *s* XPS spectrum of the as-deposited carbon film. The spectrum was decomposed into four components (blue line) using Gaussian-Lorentz functions. The two main components around 284.4 and 285.3 eV correspond to sp^2 and sp^3 carbon hybridization, respectively [24]. The remaining two components around 286.6 and 288.8 eV are attributed to carbon atoms bonded to oxygen. By comparing the relative area of sp^2 and sp^3 peaks, the sp^2/sp^3 ratio of the as-deposited film was calculated as 2.89, indicating that the carbon film is sp^2-rich.

Figure 7 shows the sp^2/sp^3 ratio and electrical conductivity of carbon films as functions of annealing temperature. The standard deviations of sp^2/sp^3 ratio and electrical conductivity aroused from the five repeated decompositions of XPS spectrum and five repeated measurements of electrical conductivity, respectively. Upon annealing at 1,000 °C, the sp^2/sp^3 ratio and electrical conductivity increased dramatically. These variations were generally considered to be caused by the thermally induced conversion from sp^3 bonds

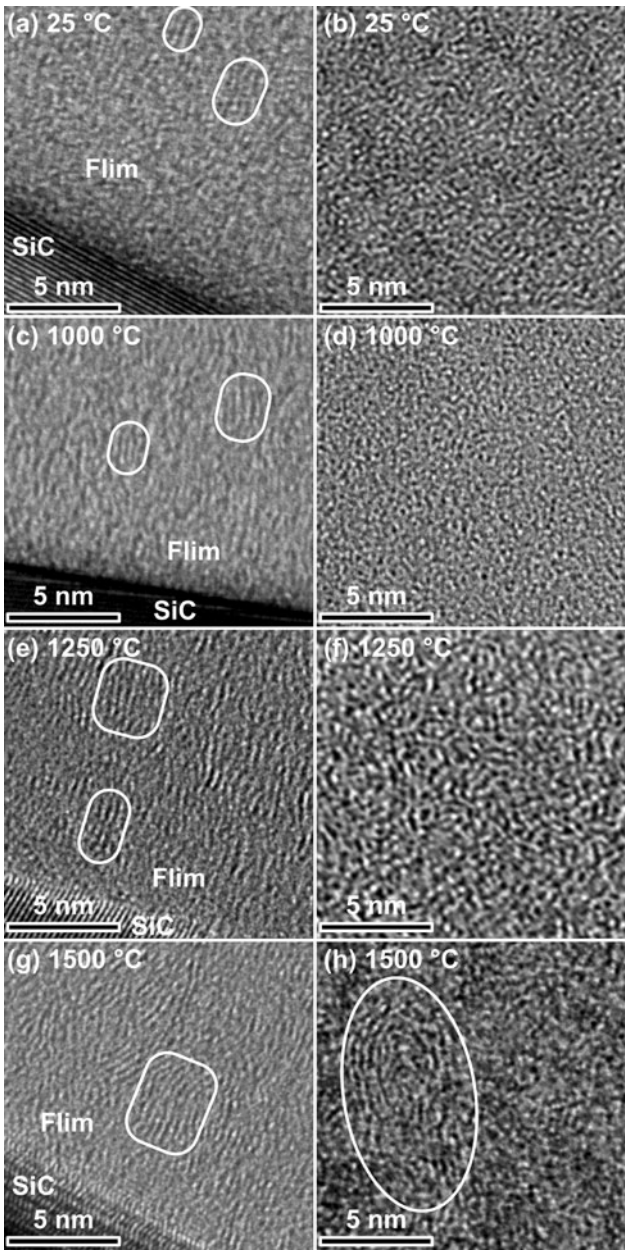

Fig. 4 Cross sectional view TEM images of **a** the as-deposited carbon film and after annealing at **c** 1,000 °C, **e** 1,250 °C and **g** 1,500 °C. Plan view TEM images of **b** the as-deposited carbon film and after annealing at **d** 1,000 °C, **f** 1,250 °C and **h** 1,500 °C

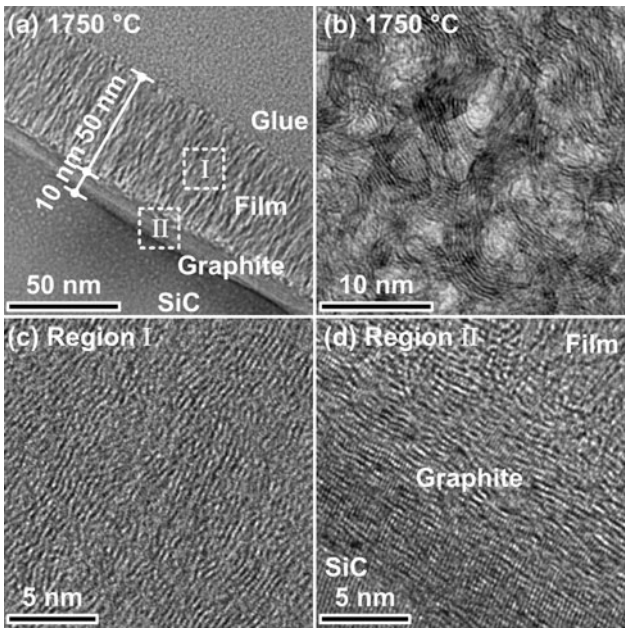

Fig. 5 TEM images of the film annealed at 1,750 °C: **a** cross sectional view, **b** plan view, **c** bulk of the carbon film (shown as I in a) and **d** graphite interlayer (shown as II in a)

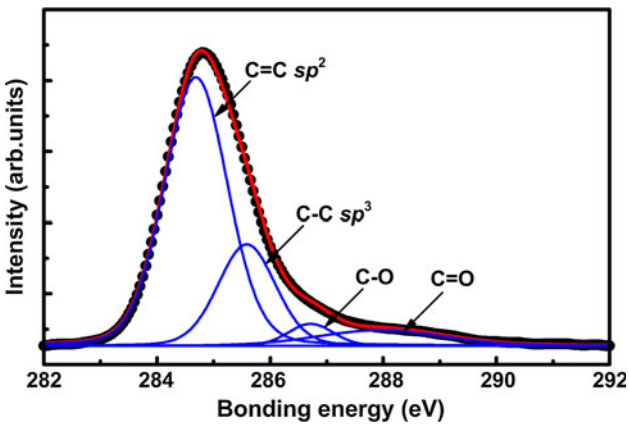

Fig. 6 C 1*s* XPS spectrum of the as-deposited carbon film (*black dotted curve*). *Blue curves*: four components; *red curve*: fitting result

to sp^2 bonds and the clustering of sp^2 bonds. It should be noted that the electrical conductivity correlates with the content of π electron in the carbon film. On one hand, the presence of sp^3 bonds could act as defects and induce strains to the sp^2 networks, resulting in the destruction of the hexagonal π-conjugated network [25]. On the other hand, clustering of sp^2 bonds promotes the formation of π electronic structure, which provides a current path in the film. When the annealing temperature was increased up to 1,500 °C, both sp^2/sp^3 ratio and electrical conductivity increased slightly. It could be inferred that the number of tubular-like structures appeared in the film at this temperature was not large, which is consistent with the results revealed by TEM in Fig. 4h. Moreover, an obvious increase of electrical conductivity at 1,750 °C is observed. This was attributed to the abundant formation of tubular-like structures and the appearance of a graphitic interlayer between the film and substrate, as revealed by TEM images in Fig. 5.

4 Discussion

During the tribotests, the decreasing process of friction coefficient was observed for the carbon films annealed

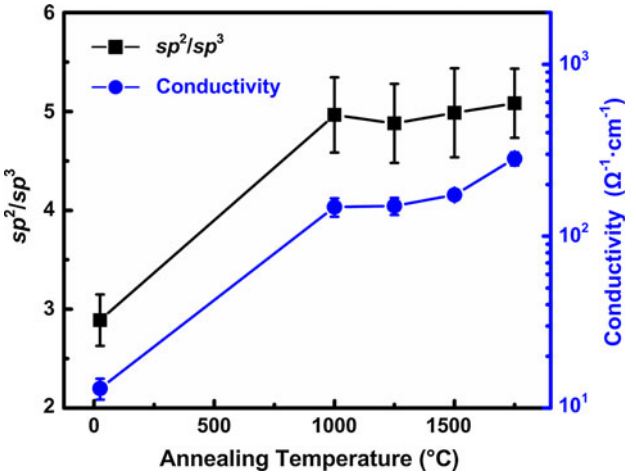

Fig. 7 sp^2/sp^3 and electrical conductivity of the carbon films as functions of annealing temperature

below 1,500 °C. In our previous work [19], we found that the inception of the friction coefficient decreasing is associated with the structure of carbon film in tribological test. In this study, the as-deposited carbon film was embedded with vertically aligned graphene sheets stacks. It should be noted that graphene sheet is the strongest in the 2D structures ever known. Thus, graphene sheets stacks would be peeled off in forms of single or multi sheets rather than be worn in a mild homogeneous process in the tribotests. The detached graphene sheets may orient toward the sliding direction and act as good solid lubricants [26], which gave rise to a lower friction coefficient. We think that the low friction mechanism induced by the graphene sheets is due to the transition of shear interactions from strong covalent bonds (between original contact surfaces) to the weak van der Waals force (between graphene sheets). Therefore, the peeling off of graphene sheets stacks governs the occurrence of friction coefficient decreasing during the sliding process. In addition, a larger size of embedded graphene sheets stack implies a stronger constraining effect by the surrounding carbon matrix. Hence, more sliding cycle is required for the stack to be peeled off by reducing such constraining effect. As a result, the sliding cycle for the friction of carbon film reaching stable increases with the annealing temperature.

In general, the sp^3 fraction controls the mechanical properties of carbon films. While in this study, although the sp^3 fraction decreased significantly at 1,000 °C (see Fig. 7), the wear life and nanoscratch depth of carbon films kept relatively constant up to 1,250 °C (see Fig. 2). Moreover, the basic nanostructure of the carbon film was maintained up to 1,250 °C with a small size increase of graphene sheets stacks mainly along the direction perpendicular to the substrate (see Fig. 4). These indicate that the wear life and nanoscratch hardness are not mainly determined by sp^3 fraction, but by the basic nanostructure of the carbon film. Furthermore, the decrease of wear life and the increase of nanoscratch depth were observed along with the appearance of few tubular-like structures in the carbon film after annealed at 1,500 °C (see Figs. 2, 4h). The formation of tubular-like structure is the result of growth and join-together of graphene sheets stacks, and it implies the lateral size increase of sp^2 nanocrystallite in the directions parallel to the substrate. Then, it is believed that the tribological properties of carbon film are more sensitive to the lateral growth of sp^2 nanocrystallite.

Besides, the temperature for formation of the graphitic interlayer between carbon film and SiC substrate was 1,750 °C (see Fig. 5a, d). It was about four hundred degrees higher than that for graphene growth on the Si-terminated 4H-SiC (0001) in ultrahigh vacuum [27]. It is because that the carbon film at the surface of SiC substrate acted as a barrier layer, which reduced the evaporation rate of Si and kept the structural stability of SiC substrate, giving better tribological properties of carbon film after annealing up to 1,500 °C.

5 Conclusion

Tribological thermostability of the carbon film with vertically aligned graphene sheets was investigated through studying the evolutions of nanoscratch depth, friction coefficient, wear life, and nanostructure as functions of annealing temperature. The results demonstrated that the tribological properties of the carbon film were thermally stable up to 1,250 °C. After annealing at 1,500 °C, the increases of friction coefficient and nanoscratch depth and the decrease of wear life were attributed to the initiation of the tubular-like structures originated from the graphene sheets stacks in the film. And after annealing at 1,750 °C, tribological performances degraded drastically as a result of the formations of abundant tubular-like structures in the carbon film and the graphitic interlayer between the film and the substrate.

Acknowledgments The authors would like to thank the National Nature Science Foundation of China (Grant No. 90923027, 51175405).

References

1. Charitidis, C.A.: Nanomechanical and nanotribological properties of carbon-based thin films: a review. Int. J. Refract. Met. Hard Mater. **28**, 51–70 (2010)
2. Grierson, D.S., Carpick, R.W.: Nanotribology of carbon-based materials. Nanotoday **2**, 12–21 (2007)
3. Donnet, C., Erdemir, A.: Solid lubricant coatings: recent developments and future trends. Tribol. Lett. **17**, 389–397 (2004)

4. Li, H.X., Xu, T., Wang, C.B., Chen, J.M., Zhou, H.D., Liu, H.W.: Annealing effect on the structure, mechanical and tribological properties of hydrogenated diamond-like carbon films. Thin Solid Films **515**, 2153–2160 (2006)
5. Wang, Z., Wang, C.B., Wang, Q., Zhang, J.Y.: Annealing effect on the microstructure modification and tribological properties of amorphous carbon nitride films. J. Appl. Phys. **104**, 073306 (2008)
6. Ferrari, A.C., Kleinsorge, B., Morrison, N.A., Hart, A., Stolojan, V., Robertson, J.: Stress reduction and bond stability during thermal annealing of tetrahedral amorphous carbon. J. Appl. Phys. **85**, 7191–7197 (1999)
7. Grierson, D.S., Sumant, A.V., Konicek, A.R., Friedmann, T.A., Sullivan, J.P., Carpick, R.W.: Thermal stability and rehybridization of carbon bonding in tetrahedral amorphous carbon. J. Appl. Phys. **107**, 033523 (2010)
8. Hirono, S., Umemura, S., Tomita, M., Kaneko, R.: Superhard conductive carbon nanocrystallite films. Appl. Phys. Lett. **80**, 425–427 (2002)
9. Shakerzadeh, M., Teo, E.H.T., Sorkin, A., Bosman, M., Tay, B.K., Su, H.: Plasma density induced formation of nanocrystals in physical vapor deposited carbon films. Carbon **49**, 1733–1744 (2011)
10. Teo, E.H.T., Kulik, J., Kauffmann, Y., Kalish, R., Lifshitz, Y.: Nanostructured carbon films with oriented graphitic planes. Appl. Phys. Lett. **98**, 123104 (2011)
11. Lau, D.W.M., Moafi, A., Taylor, M.B., Partridge, J.G., McCulloch, D.G., Powles, R.C., McKenzie, D.R.: The structural phases of non-crystalline carbon prepared by physical vapour deposition. Carbon **47**, 3263–3270 (2009)
12. McCulloch, D.G., Peng, J.L., McKenzie, D.R., Lau, S.P., Sheeja, D., Tay, B.K.: Mechanisms for the behavior of carbon films during annealing. Phys. Rev. B. **70**, 085406 (2004)
13. Marks, N.A., Cover, M.F., Kocer, C.: Simulating temperature effects in the growth of tetrahedral amorphous carbon: the importance of infrequent events. Appl. Phys. Lett. **89**, 131924 (2006)
14. McCulloch, D.G., Marks, N.A., McKenzie, D.R., Prawer, S.: Molecular dynamics and experimental studies of preferred orientation induced by compressive stress. Nucl. Instrum. Method B. **106**(1–4), 545–549 (1995)
15. Teo, E.H.T., Bolker, A., Kalish, R., Saguy, C.: Nano-patterning of through-film conductivity in anisotropic amorphous carbon induced using conductive atomic force microscopy. Carbon **49**, 2679–2682 (2011)
16. Shakerzadeh, M., Samani, M.K., Khosravian, N., Teo, E.H.T., Bosman, M., Tay, B.K.: Thermal conductivity of nanocrystalline carbon films studied by pulsed photothermal reflectance. Carbon **50**, 1422–1444 (2012)
17. Tsuchitani, S., Kaneko, R., Hirono, S.: Annealing-induced modification of superhard conductive carbon film. Jpn. J. Appl. Phys. **45**, 7036–7043 (2006)
18. Fan, X., Diao, D.F., Wang, K., Wang, C.: Multi-functional ECR plasma sputtering system for preparing amorphous carbon and Al–O–Si films. Surf. Coat. Technol. **206**, 1963–1970 (2011)
19. Wang, C., Diao, D.F.: Cross-linked graphene layer embedded carbon film prepared using electron irradiation in ECR plasma sputtering. Surf. Coat. Technol. **206**, 1899–1904 (2011)
20. Wang, C., Diao, D.F.: Graphene sheets embedded carbon film prepared by electron irradiation in electron cyclotron resonance plasma. Appl. Phys. Lett. **100**, 231909 (2012)
21. Ferrari, A.C., Robertson, J.: Interpretation of Raman spectra of disordered and amorphous carbon. Phys. Rev. B. **61**, 14095–14106 (2000)
22. Ferrari, A.C., Meyer, J.C., Scardaci, V., Casiraghi, C., Lazzeri, M., Mauri, F., Piscanec, S., Jiang, D., Novoselov, K.S., Roth, S., Geim, A.K.: Raman spectrum of graphene and graphene layers. Phys. Rev. Lett. **97**, 187401 (2006)
23. Huang, H., Chen, W., Chen, S., Wee, A.T.S.: Bottom-up growth of epitaxial graphene on 6H-SiC(0001). ACS Nano **2**, 2513–2518 (2008)
24. Diaz, J., Paolicelli, G., Ferrer, S., Comin, F.: Separation of the sp^3 and sp^2 components in the C1*s* photoemission spectra of amorphous carbon films. Phys. Rev. B. **54**, 8064–8069 (1996)
25. Takai, K., Oga, M., Sato, H., Enoki, T., Ohki, Y., Akira, T., Suenaga, K., Iijima, S.: Structure and electronic properties of a nongraphitic disordered carbon system and its heat-treatment effects. Phys. Rev. B. **67**, 214202 (2003)
26. Dienwiebel, M., Verhoeven, G.S., Pradeep, N., Frenken, J.W.M., Heimberg, J.A., Zandbergen, H.W.: Superlubricity of graphite. Phys. Rev. Lett. **92**, 126101 (2004)
27. Lu, W., Boeckl, J.J., Mitchel, W.C.: A critical review of growth of low-dimensional carbon nanostructures on SiC (0001): impact of growth environment. J. Phys. D. **43**, 374004 (2010)